

## Analysis and Experiment of the Performance of a Flat-Plate Solar Collector Considering of the Wavelength Dependence\*

by Kimio KANAYAMA\*\* and Hiromu BABA\*\*

(Received April 30, 1988)

### Abstract

Taking into consideration the wavelength dependence of the spectral radiative characteristics of an absorbing plate and a transparent plate which are the main components of a flat-plate solar collector, the performance of the solar collector was analyzed from the view point of the heat balance on the absorbing and transparent plates based mainly on the radiation heat transfer under the steady state. Two sorts of handmade solar collectors with selective and non-selective wavelength characteristics were constructed to compare the analytical result with a long term experiment outdoors.

Comparison of the calculations with the measurements showed them to be in fairly good agreement for both the selective and the non-selective collectors, and it was thus shown that the prediction method could generally be applied to evaluate the collector's performance.

### 1. Introduction

The leading research on the performance of a flat-plate solar collector is the old paper by Hottel et al.<sup>1)</sup>, and recently details of a procedure to predict the performance of a solar collector have been reported by Whillier<sup>2)</sup>. In these researches, respecting the radiative properties of the absorbing and transparent plates of the solar collector, however, the wavelength dependence of the spectral radiative characteristics for solar radiation was not considered. On the other hand, a flat-plate solar collector which is composed of a selective absorbing plate such as black chrome and a selective transparent plate such as a glass plate is in actual fact used in order to improve the collection efficiency of solar energy. Therefore, the authors<sup>3),4)</sup> have carried forward the analyses and experiments with the performance of the flat-plate solar collector considering the wavelength dependence of the transparent and absorbing plates.

From among many fundamental approaches to evaluate the performance of solar collectors, the distinguished measurements of collector performance were vigorously carried out by the NASA-Lewis Research Center<sup>5),6)</sup> both indoors and outdoors, and various testing methods were proposed in detail by Hill et al.<sup>7)</sup> to point toward the adoption of a standard test method for testing and rating collectors.

\* This paper was presented at the 21st National Heat Transfer Symposium of Japan, 1984, (Kyoto).

\*\* Department of Mechanical Engineering, Kitami Institute of Technology.

In this paper, the heat balance on the absorbing plate and the transparent plate which are the main parts of a solar collector was considered for analysis, and an evaluation of the collector's performance at steady state was made taking into account their spectral wavelength dependence. Moreover, the results predicted by the calculation were verified by a long term outdoor experiment using a handmade solar collector.

## 2. Analytical Method

Referring to the relationship of heat transfer within the model of the solar collector shown in Fig. 1, the equations of heat balance on an absorbing plate and a transparent plate are as follows:

$$(Q_{PA1} + Q_{PA2} + Q_{PA3}) - (Q_{PCV} + Q_{PR} + Q_{PCD} + Q_{PW}) = 0 \quad (1)$$

On the transparent plate;

$$(Q_{GA1} + Q_{GA2} + Q_{GA3} + Q_{GA4} + Q_{PCV}) - (Q_{GR} + Q_{GCVO} + Q_{GRO}) = 0 \quad (2)$$

There is the research<sup>8)</sup> dealing with the problem to be non-steady, because the temperatures of the absorbing and transparent plates are minutely varied in relation to the heat capacity of the collector system, the meteorological conditions for solar radiation, and so on. On a clear day, however, it is assumed that the phenomena scarcely change during a short period, and the calculation is treated as being under the quasi-steady condition in this analysis. Considering the spectral absorptance and emittance of the absorbing plate, and the spectral transmittance of the transparent plate, all the radiation components are integrated over the wavelength, that is, every  $0.02 \mu\text{m}$  from  $0.36 \sim 1.0 \mu\text{m}$  of wavelength and every  $0.2 \mu\text{m}$  for the range from  $1 \sim 25 \mu\text{m}$  of wavelength, and furthermore the spectral distribution of solar radiation is also integrated by the same wavelength pitches as shown above under the assumed air mass<sup>9)</sup>. The calculation method of the heat balance is essentially the same as that of the repeat calculation by Duffie and Beckman<sup>10)</sup> and Tanaka<sup>11)</sup>. Firstly, the following values; solar radiation  $Q_0 (= A_c J)$ , air mass  $m$ , ambient temperature  $t_a$ , wind velocity  $v$ , water temperature at the inlet pipe of the collector  $t_{wen}$ , flow rate of the water  $G$ , inclination

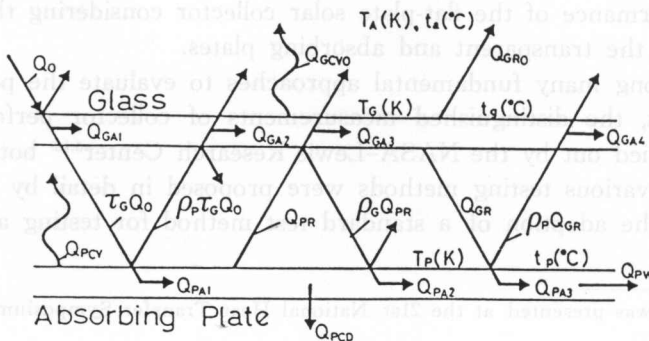


Fig. 1. Heat transfer mechanism in the solar collector model.

angle of the collector  $\theta$ , heat loss factor from the side wall of the collector  $F_L$  are given for the calculation of Eqs. (1) and (2). After the initial temperatures of the glass  $t_g$  and the absorbing plate  $t_p$  are given to be equal to  $t_a$  and  $t_{wen}$  respectively, both values of  $t_g$  and  $t_p$  are gradually increased independently until the equilibrium of Eq. (2) is attainable beforehand, and then when the equilibrium of Eq. (1) can be attained so repeatedly that the conditions of Eq. (3) and Eq. (4) are satisfied, the calculation comes to an end.

With respect to the conditions between the absorbing plate and the water, the heat absorbed by the water from the absorbing plate,  $Q'_{pw}$ , is

$$Q'_{pw} = c_w G (t'_p - t_{wen}) (1 - e^{-KW_0 L_0 / c_w G}) \quad (3)$$

where,  $c_w$  is the specific heat of the water,  $G$  is the flow rate of the water,  $K$  is the total heat conductance between the absorbing plate and the water,  $W_0$  is the width of the absorbing plate,  $L_0$  is the length of the absorbing plate.

On the other hand, the heat transported by the water flowing through the collector tubes,  $Q''_{pw}$ , is caused by the difference between the water temperatures at the outlet and the inlet pipes of the collector, and thus  $Q''_{pw}$  is

$$Q''_{pw} = c_w G (t_{wex} - t_{wen}) \quad (4)$$

Under the temperature of the absorbing plate  $t_p$  assumed beforehand, the initial value of the water temperature of the outlet  $t_{wex}$  is fixed to be equal to the water temperature of the inlet  $t_{wen}$ , and when the condition of Eq. (3)=Eq. (4) is satisfied by increasing  $t_{wex}$  gradually, then  $t_{wen}$  and  $t_{wex}$  can be determined. In this case, as  $Q'_{pw}$  must be equal to  $Q''_{pw}$  and furthermore the heat collected by the collector,  $Q_{pw}$ , calculated by Eq. (1) must be equal to both  $Q'_{pw}$  and  $Q''_{pw}$ , so the condition that  $Q_{pw} = Q'_{pw} = Q''_{pw}$  is required. Therefore, by comparing the temperatures of the absorbing plate  $t_p$  with  $t'_p$ , the calculation is repeated until the difference between both converges below  $\pm 0.1^\circ\text{C}$ , and when this is satisfied it is considered that equilibrium can finally be attained. Consequently,  $t_p$ ,  $t_g$ ,  $t_{wen}$  and  $t_{wex}$  are determined, and the collector efficiency  $\eta_{ct}$  can be calculated by

$$\eta_{ct} = Q_{pw} / Q_0 = c_w G (t_{wex} - t_{wen}) / A_c J \quad (5)$$

where,  $A_c$  is the effective area of the collector, and  $J$  is the solar radiation.

Next, the contents of each term of Eqs. (1) and (2) are as follows: The heat absorbed by the absorbing plate from the solar radiation incident upon the collector,  $Q_{PA1}$ , is

$$Q_{PA1} = \sum \{ \alpha_{p\lambda} \tau_{g\lambda} A_c J / (1 - \rho_{p\lambda} \rho_{g\lambda}) \} \Delta F_\lambda(m)$$

Similarly, the heat reabsorbed by the absorbing plate from the radiation emitted by itself,  $Q_{PA2}$ ;

$$Q_{PA2} = \sum \{ \alpha_{p\lambda} \varepsilon_{p\lambda} \sigma T_p^4 A_c / (1 - \rho_{p\lambda} \rho_{g\lambda}) \} \Delta F_\lambda(T_p)$$

The heat absorbed by the absorbing plate from the radiation emitted by the glass plate,  $Q_{PA3}$ ;

$$Q_{PA3} = \sum \left\{ \alpha_{p\lambda} \varepsilon_{p\lambda} \sigma T_G^4 A_c / (1 - \rho_{p\lambda} \rho_{g\lambda}) \right\} \Delta F_\lambda(T_G)$$

The heat absorbed directly by the glass plate from the solar radiation incident upon the collector surface,  $Q_{GA1}$ ;

$$Q_{GA1} = \sum \alpha_{g\lambda} A_c J \Delta F_\lambda(m)$$

The heat absorbed by the glass plate from the solar radiation incident through it and reflected on the absorbing plate,  $Q_{GA2}$ ;

$$Q_{GA2} = \sum \left\{ \alpha_{g\lambda} \rho_{p\lambda} \tau_{g\lambda} A_c J / (1 - \rho_{p\lambda} \rho_{g\lambda}) \right\} \Delta F_\lambda(m)$$

The heat absorbed by the glass plate from the radiation emitted by the absorbing plate,  $Q_{GA3}$ ,

$$Q_{GA3} = \sum \left\{ \alpha_{g\lambda} \varepsilon_{p\lambda} \sigma T_P^4 A_c / (1 - \rho_{p\lambda} \rho_{g\lambda}) \right\} \Delta F_\lambda(T_P)$$

The heat reabsorbed by the glass plate from the radiation emitted by itself,  $Q_{GA4}$ ;

$$Q_{GA4} = \sum \left\{ \alpha_{g\lambda} \rho_{p\lambda} \varepsilon_{g\lambda} \sigma T_G^4 A_c / (1 - \rho_{p\lambda} \rho_{g\lambda}) \right\} \Delta F_\lambda(T_G)$$

The heat loss by radiation from the top surface of the solar collector,  $Q_{GRO}$ ;

$$Q_{GRO} = \sum \varepsilon_{g\lambda} \sigma T_G^4 A_c \Delta F_\lambda(T_G) - \sum \alpha_{g\lambda} \sigma T_A^4 A_c \Delta F_\lambda(T_A)$$

The heat transmitted by convection through the air layer between the absorbing and transparent plates,  $Q_{PCV}$ ;

$$Q_{PCV} = C(t_p - t_g) A_c$$

The heat loss by convection from the top surface of the collector,  $Q_{GCVO}$ ;

$$Q_{GCVO} = K_0(t_g - t_a) A_c$$

And the heat loss from the back surface of the collector,  $Q_{PCD}$ ;

$$Q_{PCD} = K_u(t_p - t_a) A_c F_L$$

Where,  $\alpha_{p\lambda}$ ,  $\varepsilon_{p\lambda}$  and  $\rho_{p\lambda}$  are the spectral absorptance, emittance and reflectance of the absorbing plate respectively.  $\alpha_{g\lambda}$ ,  $\varepsilon_{g\lambda}$ ,  $\rho_{g\lambda}$  and  $\tau_{g\lambda}$  are the spectral absorptance, emittance, reflectance and transmittance of the transparent plate respectively.  $\sigma$  is a Stefan-Boltzmann constant.  $\Delta F_\lambda(m)$ ,  $\Delta F_\lambda(T_p)$ ,  $\Delta F_\lambda(T_g)$  are the energy rates of solar radiation with air mass  $m$ , of the blackbody radiation emitted from the absorbing plate of temperature  $T_p$ (K) and of the blackbody radiation emitted from the transparent plate of temperature  $T_g$ (K) at wavelength  $\lambda$  respectively.  $C$  is the heat transfer coefficient of the air layer within the solar collector.  $K_0$  and  $K_u$  are the heat conductances on the top and back surfaces of the solar collector.

### 3. The Results of Calculation

#### 3.1. Solar collector with selective characteristics

The selective characteristics of the spectral absorptance and emittance of the absorbing plate, the spectral transmittance of the transparent plate (glass), and the

spectral energy distribution of solar radiation of several air masses used for the calculation are shown in Fig. 2. The collection efficiency calculated is shown in Fig. 3, under the conditions that solar radiations are 300~700 kcal/m<sup>2</sup>h (1256~2931 Jk/m<sup>2</sup>h, 349~814 W/m<sup>2</sup>), air mass  $m=1$ , ambient temperatures are 0, 10, 20 and 30°C, wind velocity is 0.5 m/sec, inclination angle of the solar collector is 45°, and fractions of the heat loss from the side wall of the collector (=heat loss factor  $F_L$ ) are 1.2, 1.5 and 1.8. In this Figure, each efficiency curve for

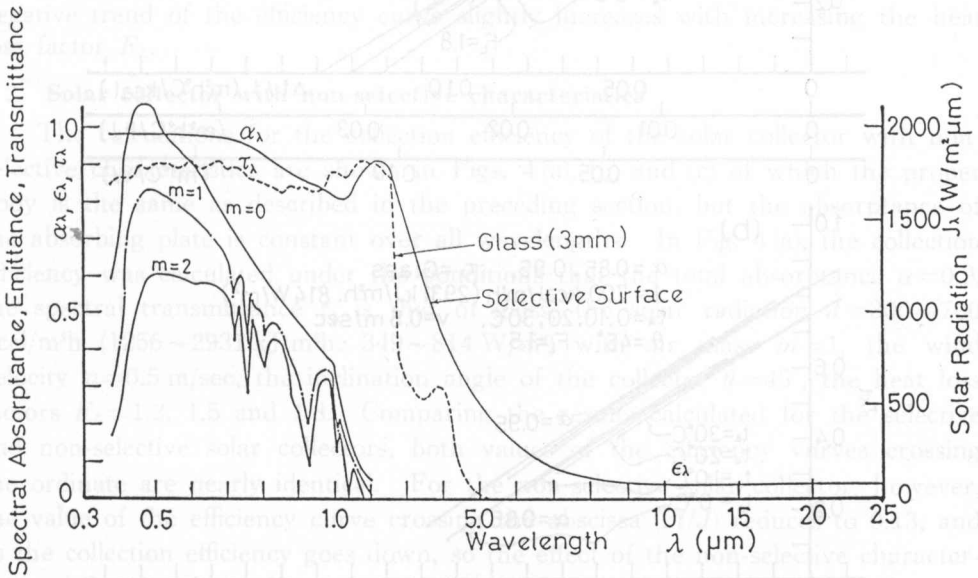


Fig. 2. Wavelength dependences of radiative properties of glass and selective surface, and energy distribution of solar radiation.

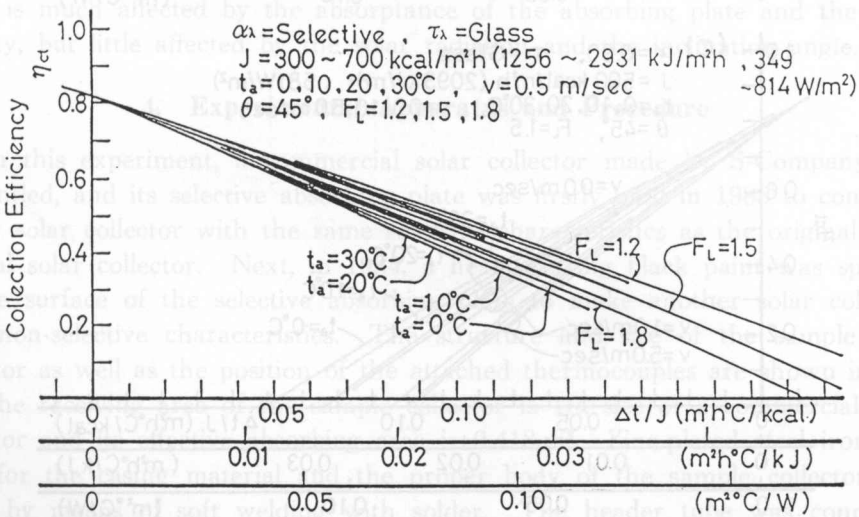
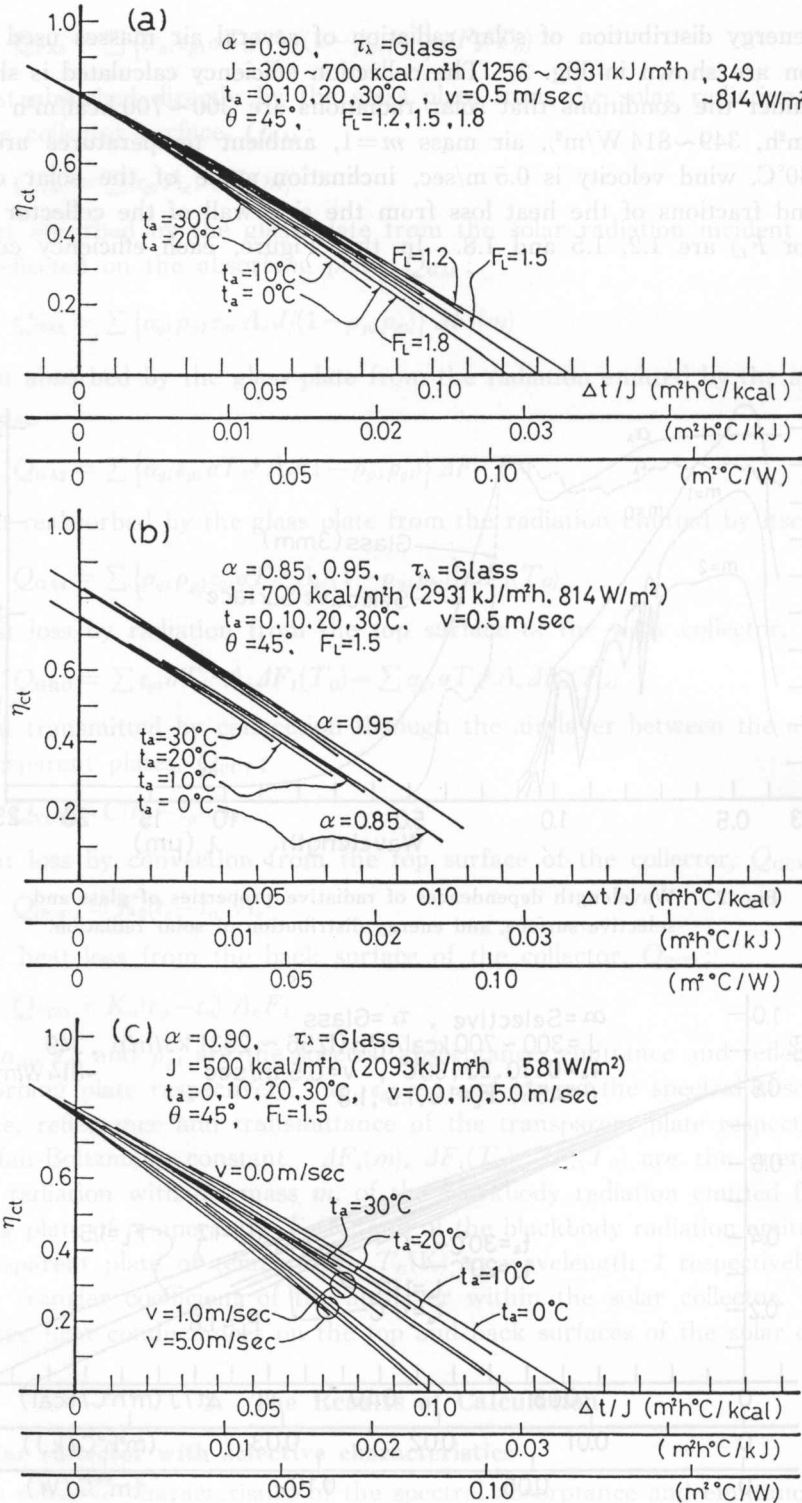


Fig. 3. Collector efficiency calculated for the selective solar collector.



Figs. 4(a), (b) and (c). Collection efficiencies calculated for the non-selective solar collector.

these three heat loss factors is not just indicated by a line, but by a bundle of many lines which are over all ranges of  $(\Delta t/J)$  of the abscissa when varying the values of both solar radiation  $J$  and outside temperature  $t_a$ .

Each bundle of these lines is convex upward with a slightly negative trend and spreads like a broom from one point of small negative value of  $(\Delta t/J)$  with increasing  $(\Delta t/J)$ . As it has the large values of 0.8 of  $\eta_{ct}$  crossing the ordinate and 0.2 of  $(\Delta t/J)$  crossing the abscissa, the effect of the selective characteristics of the absorbing and transparent plates can clearly be seen. However, the negative trend of the efficiency curve slightly increases with increasing the heat loss factor  $F_L$ .

### 3.2. Solar collector with non-selective characteristics

The calculations for the collection efficiency of the solar collector with non-selective characteristics are shown in Figs. 4(a), (b) and (c) of which the proper body is the same as described in the preceding section, but the absorptance of the absorbing plate is constant over all wavelengths. In Fig. 4(a), the collection efficiency was calculated under the conditions that the total absorptance  $\alpha=0.9$ , the spectral transmittance  $\tau_\lambda$  is that of glass, the solar radiation  $J=300\sim 700$  kcal/m<sup>2</sup>h (1256~2931 kJ/m<sup>2</sup>h, 349~814 W/m<sup>2</sup>) with air mass  $m=1$ , the wind velocity  $v=0.5$  m/sec, the inclination angle of the collector  $\theta=45^\circ$ , the heat loss factors  $F_L=1.2, 1.5$  and  $1.8$ . Comparing the results calculated for the selective and non-selective solar collectors, both values of the efficiency curves crossing the ordinate are nearly identical. For the non-selective solar collector, however, the value of the efficiency curve crossing the abscissa  $(\Delta t/J)$  reduces to 0.13, and as the collection efficiency goes down, so the effect of the non-selective characteristics of the absorbing plate can clearly be seen. Each of the collection efficiency curves gathered like a bundle is also convex upward with a steeper slope than that of the selective collector. Also, as shown in Figs. 4(b) and (c) the efficiency curve is much affected by the absorptance of the absorbing plate and the wind velocity, but little affected by the solar radiation and the inclination angle.

## 4. Experimental Apparatus and Procedure

In this experiment, a commercial solar collector made by S-Company was dismantled, and its selective absorbing plate was firstly used in 1983 to construct a new solar collector with the same selective characteristics as the original commercial solar collector. Next, in 1984, a heat resisting black paint was sprayed on the surface of the selective absorbing plate to make another solar collector with non-selective characteristics. The structure and size of the sample solar collector as well as the position of the attached thermocouples are shown in Fig. 5. The receiving area of the sample collector is 1/4 size of a commercial solar collector and its effective absorbing area is 0.418 m<sup>2</sup>. Zinc-plated steel iron was used for the casing material and the proper body of the sample collector was made by means of soft welding with solder. The header tube was connected to the absorbing tube by means of hard welding with silver alloy. A 3 mm

thick normal glass was used as the transparent plate fixed onto the casing with small screws by medium of an aluminum sash, and the gap between the glass and the aluminum sash was sealed with silicon bond. The bottom of the solar

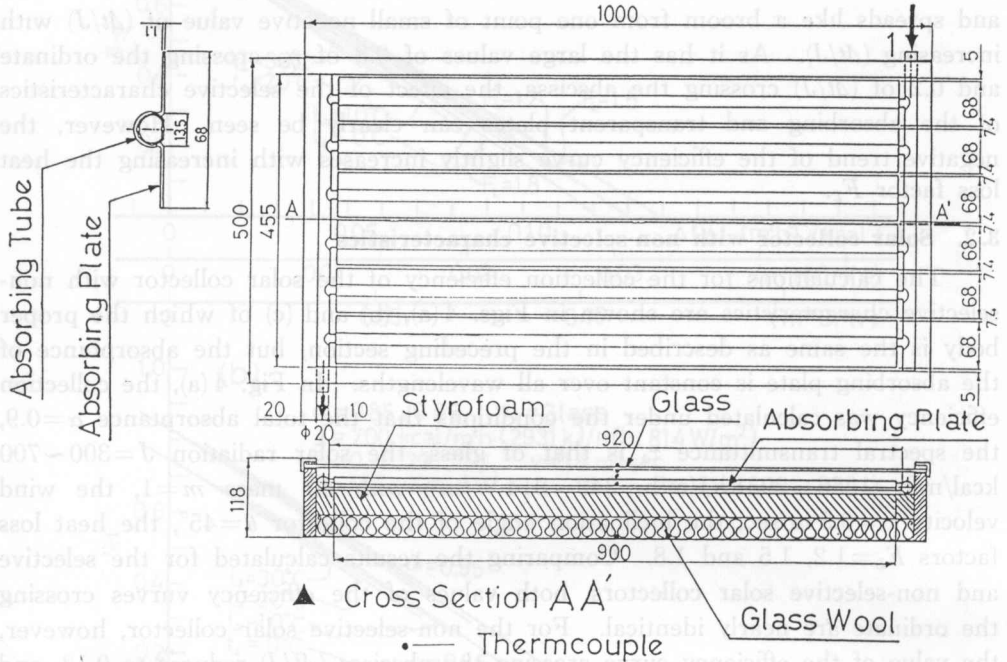


Fig. 5. Details of the handmade solar collector.

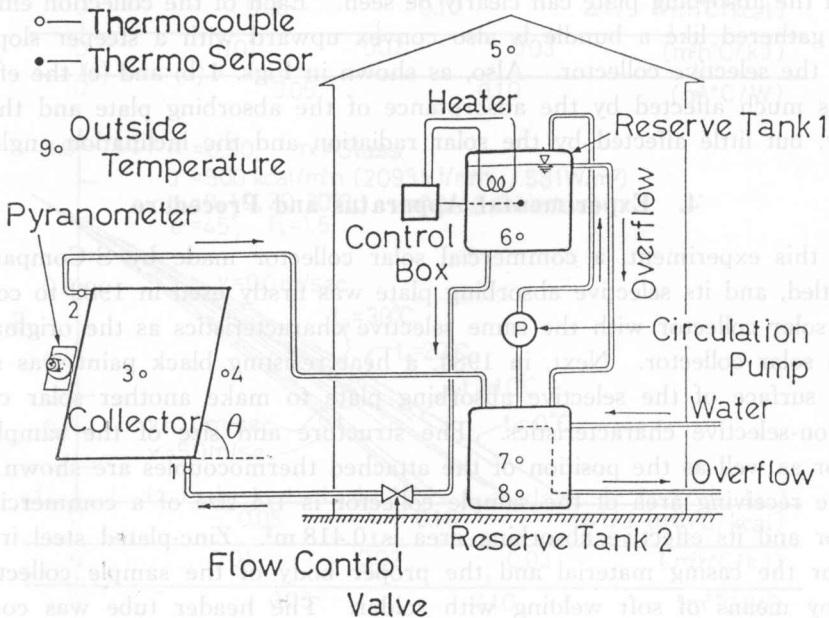


Fig. 6. Schematic diagram of the experimental apparatus.

collector was insulated by a 75 mm thick layer in total composed of 35 mm thick glass wool and 40 mm thick styrofoam, and the side wall of the collector was also insulated by 20 mm thick glass wool.

Figure 6 is a block diagram of the experimental apparatus. With respect to the operation procedure of the apparatus, water that flows down from the header tank (Reserve tank 1) due to gravity is fed to the sample collector through the inlet pipe. The water that is warmed while passing through the inside of the collector flows out from the outlet pipe, goes to the auxiliary tank (Reserve tank 2) and is then pumped up to the header tank again. In order to prevent the over feed of the water, an overflow pipe was devised on the header tank in this apparatus. Pipe made from polychloride vinyl was used for the piping and the outside of the pipe lines and the tanks were strictly insulated.

For the measurement of the temperature at various parts of the apparatus, thermocouple detectors were placed at each point shown in Figs. 5 and 6. Hence, the points used to measure the temperature were as follows: the inlet and outlet pipes of the collector, the front and back surfaces of the glass plate, the air layer between the glass and the absorbing plates, the surface of the absorbing plate, the insulation layer of the collector bottom, the center of the header tank, the center and bottom of the auxiliary tank, and the outside and inside of the room. The measurement of these temperatures was carried out every 30 minutes from AM 9:00 to PM 3:00 on a clear day, and the values measured over 1.5 or 2.0 hours in the middle of solar noon were available for the data.

For the measurement of the flow rate, the weight of the water received in a beaker for a fixed period was measured at the inlet pipe of the auxiliary tank after flowing out of the collector. The rate of the water circulated through the collector was controlled by a globe valve in four flow ranges of 75, 84, 111 and 120 kg/h.

In order to accurately measure the solar radiation, a pyranometer (EKO MS-42) was placed on the surface with the same inclination angle as the solar collector and the solar radiation was obtained as the value integrated for every 30 minutes.

## 5. Experimental Results and Discussion

### 5.1. Solar collector with selective characteristics

Figure 7 shows the experimental results obtained from July to November in 1983. The initial temperature of the water within the header tank was controlled in the broad range from 10 to 60°C, so that the measured points could be distributed widely over the abscissa. In this case, the flow rate of water was constantly kept at  $G=75$  kg/h. The experimental equations and curves obtained by means of the least squares method to approximate the measured results to linear and secondary lines are also shown in Fig. 7. Comparison between the experimental solid lines numerically regressed from the measurements and the calculated dashed lines transferred from Fig. 3 shows that the experimental

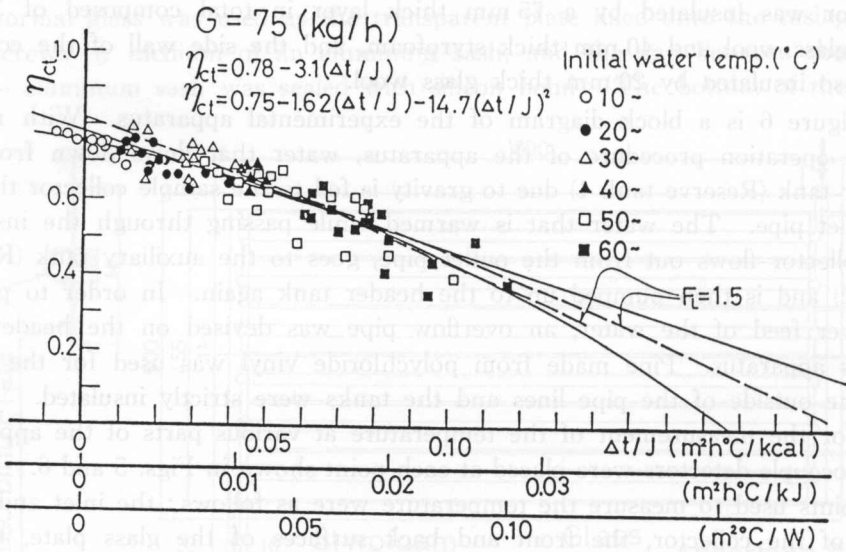


Fig. 7. Comparison between the measurements and calculations for the selective solar collector.

lines lie near both sides of two calculated lines in the case of the heat loss factor  $F_L=1.5$ , except that the latter only exceeds the former at the value crossing the ordinate.

**5. 2. Solar collector with non-selective characteristics**

Figure 8 shows the experimental results obtained from August to December in 1984 with the flow rate of the water  $G=84 \text{ kg/h}$ . The experimental equations

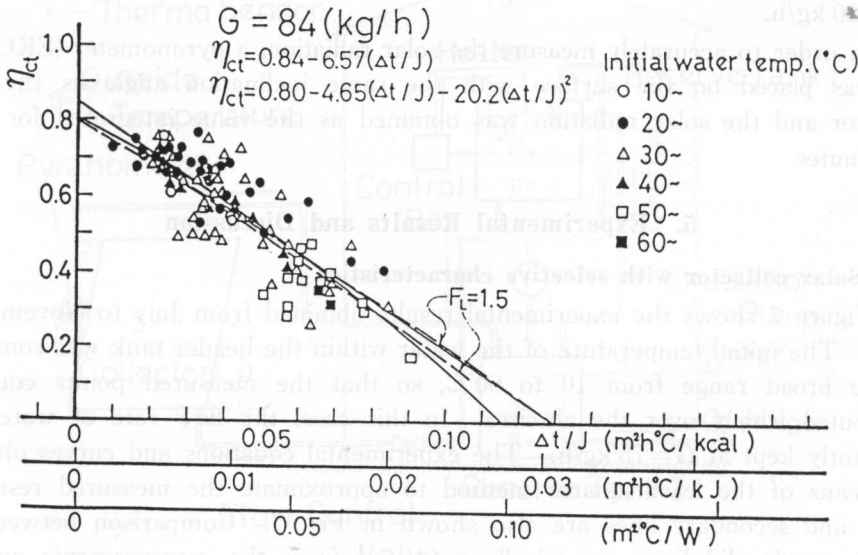


Fig. 8. Comparison between the measurements and calculations for the non-selective solar collector.

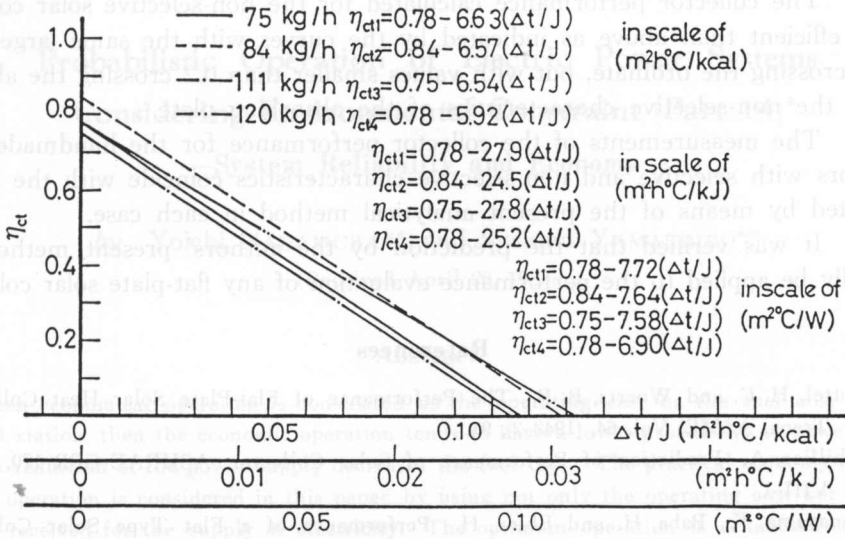


Fig. 9. Collection efficiencies for all the experimental results.

and curves approximated linearly from the measured results are also shown in the Figure. Comparing the experiments with the calculations shown in Fig. 4, the former agrees well with the latter in the case of  $\alpha=0.9$  and  $F_L=1.5$  for both the value crossing the ordinate and the inclination angle of the curve. Additionally, as shown in Fig. 9, almost the same results as above were also obtained when measured at the flow rates  $G=75, 84, 111$  and  $120$  kg/h.

Since the absorptance of the non-selective absorbing plate of the sample collector is 0.9 in the infrared region, it is supposed that the value of absorptance in the visible region may really be the same as this. The heat loss factor 1.5 which was used in these calculations approximates roughly to the value of 1.7 obtained simply as the ratio of the side wall to the bottom surface of the collector.

### 6. Conclusions

Taking into account the wavelength dependence of the spectral radiative characteristics of the absorbing and transparent plates which are the main parts of a flat-plate solar collector, the performance of the solar collector was calculated from the view point of the heat balance on both plates based mainly on the radiation heat transfer. At the same time, the measurements for the collector performance were made by using two handmade solar collectors with selective and non-selective characteristics by a long term outdoor experiment. The results obtained under normal conditions are as follows :

- 1) The collector performance calculated for the selective solar collector is more efficient because of the spectral radiative characteristics of both the absorbing and the transparent plates, as indicated by a bundle of curves with large values of 0.8 of  $\eta_{ct}$  crossing the ordinate and 0.2 of  $(\Delta t/J)$  crossing the abscissa.

2) The collector performance calculated for the non-selective solar collector is less efficient than above as indicated by the curves with the same large value of 0.8 crossing the ordinate, but with values smaller than 0.2 crossing the abscissa due to the non-selective characteristics of the absorbing plate.

3) The measurements of the collector performance for the handmade solar collectors with selective and non-selective characteristics coincide with the results calculated by means of the present analytical method in each case.

4) It was verified that the prediction by the authors' present method can generally be applied to the performance evaluation of any flat-plate solar collector.

### References

- 1) Hottel, H. C. and Woertz, B. B. The Performance of Flat-Plate Solar Heat Collector, Trans. ASME, Vol. 64, (1942-2), 91.
- 2) Whillier, A. Prediction of Performance of Solar Collector, ASHRAE GPR 170, (1977), VIII-1.
- 3) Kanayama, K., Baba, H. and Ebina, H. Performance of a Flat Type Solar Collector Composed of the Selective Transparent and Absorbing Plates, 2nd Miami International Conference on Alternative Energy Sources, Alternative Energy Sources II, Vol. 1, Solar Energy 1, (1979), 101.
- 4) Kanayama, K. and Baba, H. Performance of a Flat-Plate Solar Collector Considering Wavelength Dependence, Proc. 21st National Heat Transfer Symposium of Japan (in Japanese), 1984, Kyoto, 376.
- 5) Simon, F. F. Flat-Plate Solar-Collector Performance Evaluation with a Solar Simulator as a Basis for Collector Selection and Performance Prediction, NASA, TMX-71793, Technical Paper Presented at the 1975 International Solar Energy Society Meetings, Los Angeles, California, July 28-Aug. 8, 1975.
- 6) Vernon, R. W. Solar Collector Performance Evaluated Outdoors at NASA-Lewis Research Center, NASA TMX-71689, Proc. of the Workshop Solar Collectors for Heating and Cooling of Buildings, New York, Nov. 21-23, 1974, Report No. NSF-RA-N-75-019, University of Maryland, May, 1975.
- 7) Hill, J. E. and Streed, E. R. Testing and Rating of Solar Collectors, ASHRAE GRP 170, (1977), X-1.
- 8) Saito, A., et al. Transient Characteristics of a Collecting System on a Flat-Plate Solar Collector (in Japanese), Trans. JSME(B), 48-429, (1982-5), 934.
- 9) Moon, P. J. Frankline Inst., Vol. 230, (1940), 583.
- 10) Duffie, J. A. and Beckman, W. A. Solar Energy Thermal Process, John Wiley & Sons, (1974), 129.
- 11) Tanaka, S. Cooling and Heating Systems Using Solar Energy, Ohm, Tokyo, (1978), 82.